Graph Cut Segmentation of Sparsely Sampled Images with Application to InSAR-measured Changes in Elevation

Michael Stuecheli, Andrea Vaccari, Scott T. Acton
{mds4m, av9g, acton}@virginia.edu
Department of Electrical and Computer Engineering
University of Virginia
Charlottesville, VA 22904

***Abstract*—In this paper, we outline an algorithm for the automatic segmentation of sparse data in order to detect possible terrain-deformation phenomena. Segmentation is accomplished through a graph cut technique. In the graph structure, for each edge, we derive a unique energy by combining multiple independent energies tailored toward accurately locating the boundaries of spot-like, subsiding regions. We then find the series of cuts with minimum total energy and fit splines to these cuts for smooth segment boundaries. The segmentation approach is applied to the problem of localizing sinkholes in karst regions. Test results indicate efficacy for a sufficient density of InSAR features.**

***Inext Terms*—** Graph Cut, Segmentation, Remote Sensing

I. INTRODUCTION

Due to the ability to cover wide areas in a short time and to emerging commercial availability, remote sensing has witnessed increasing application over the last few decades. In particular RADAR (RAdio Detection And Ranging), able to operate in all-weather conditions, has seen significant development, and the range of applications has been constantly growing. Salient examples include monitoring of precursory deformation phenomena for either earthquakes or volcanoes, study of the role of glaciers and ice sheets in sea level rise, evaluation of the role of ground water, surface water, soil moisture and snow pack contribution to global fresh water budget; monitoring of Earth's vegetation structure and ocean surface, and planetary science [1,2].

The development of techniques such as Synthetic Aperture Radar (SAR) [3], Interferometric SAR (InSAR) [4], and Differential InSAR (DInSAR) [5] have resulted in the ability to produce, in a short time, large high resolution Digital Elevation Models (DEM) and track their evolution over time.

The ability to monitor surface changes over time is of high interest in the transportation community. In 2000, the damage to infrastructure due to subsidence and landslide were evaluated at $2.2 billion (US only) and $6.8 billion (globally) with a potential saving of $430 million (US only) and $1.4 billion (globally) with the implementation of remote sensing early detection and tracking (numbers are in yr. 2000 USD) [1].

Within this framework, one of the goals of our study is to verify that remote sensing can be used as a surveying tool by developing algorithms to allow early detection of subsidence regions.

II. BACKGROUND

To generate an interferogram (InSAR), two complex SAR images of the same location taken from two different vantage points are required. In this imaging scenario, each pixel (ground resolution element, typically few tens of square meters in size) of each image has a phase proportional to its distance from the satellite. Once the two images are registered with each other, the difference in phase can be used to evaluate the elevation of each pixel [4]. When several SAR images are available this process is repeated for all the possible baselines (combination of two vantage points). One of the major problems with this process is decorrelation [6]. Such decorrelation can occur for several reasons. Longer baselines cause the difference in phase between two pixels to increase until the limit where it wraps around thus sacrificing coherence. If the time between two acquisitions is significant, the pixel itself might change properties (as in case of vegetation) and cause decorrelation. Other effects might include atmospheric interference, rotation of the image, *etc*.

A new technique has been developed to address these two opposing requirements: Permanent Scatterer InSAR (PSInSAR) [7]. This method is used to statistically analyze a stack of SAR images to determine which pixels contain *permanent scatterers* (target much smaller than a pixel whose response does not significantly change in time and it is fairly constant with respect to the baselines). This technique was recently extended to include *distributed scatterers* (large regions showing similar behavior on several adjacent pixels over a subset of baselines) under the name of SqueeSAR [8].

The end result of the SqueeSAR processing is a temporal stack of sparse geo-referenced points, which serves as the starting point of our analysis.

In this paper we present a graph cut-based segmentation approach applied to the point cloud to outline subsidence regions in order to detect possible sinkholes.

This work was supported in part by U.S. Department of Transportation under Grant RITARS-11-H-UVA.

III. METHOD AND THEORY

A. Graph Cuts

A graph cut is a segmentation of an arbitrary graph via the 'cutting' of edges; the optimal cut is one which has minimum energy, given by

$$E_{cut} = \sum_{u \in A, v \in B} w(u, v) \tag{1}$$

where A and B are the disjoint sets of vertices created by the cut, and $w(u,v)$ is the weight of a given edge between vertices (u,v). Typically, the energy of a cut is expanded to include a measure of association between the 'cut' sets [9] A and B—this promotes spatial coherence, preventing small, isolated vertices from being unnecessarily cut away. This expansion is sometimes termed the normalized cut:

$$NE_{cut} = \frac{E_{cut}(A,B)}{assoc(A,V)} + \frac{E_{cut}(A,B)}{assoc(B,V)} \tag{2}$$

and

$$assoc(A,V) = \sum_{u \in A, t \in V} w(u,t) \tag{3}$$

$$assoc(B,V) = \sum_{u \in B, t \in V} w(u,t) \tag{4}$$

In (3) and (4), t is any other vertex in the set of all vertices, V. An alternative cut expression to (2) is the expression [10]

$$E_{cut}(f) = \lambda \sum_{p \in P} R_p(f_p) + \sum_{\{p,q\} \in N} B_{\{p,q\}}(f_p, f_q) \tag{5}$$

where p and q are vertices, B is the associativity term, R is the traditional energy assigned to an edge, and λ is a weighting factor.

B. Our Method

In our method, we must first construct a graph from a point cloud of data—in this application, the point cloud is a result of post-processing stacks of InSAR (interferometric synthetic aperture radar) images; this process produces non-uniform and sparsely distributed data locations. The points are taken as vertices, and the edges are created with a Delaunay triangulation. The Delaunay triangulation (in two dimensions) ensures that the circumcircle of each triangle created has an empty interior; thus this triangulation scheme maximizes the minimum angle of each triangle produced and creates non-overlapping edges, resulting in an edge construct that accurately reflects local neighborhood relationships.

Graph cuts have been used extensively in the literature in the pursuit of segmentation; however, the technique is typically applied to rasterized images which offer only intensity and pixel location information. Our dataset is unique in that it offers multiple facets of information for each point—displacement time series, coherence, velocity, acceleration, physical area represented, elevation, location, etc. So, the feature set is broadened, as are the factors which might influence the edge weights. In our initial foray into this approach, we have limited the scope of edge weight influences to those factors that might most immediately (and accurately) indicate the presence of a sinkhole-forming region:

- displacement difference between two vertices
- displacement range
- coherence

We choose to use displacement difference in place of the slope of displacement in order to separately consider (and independently weight) the length of an edge, as described later.

Next, we derive independent energies for each pertinent factor. With the aim of segmenting possible sinkhole-formation regions, we develop these energies to favor a minimum when on the boundary of such a region. Succinctly, we are searching for characteristics indicative of the edge of a spot:

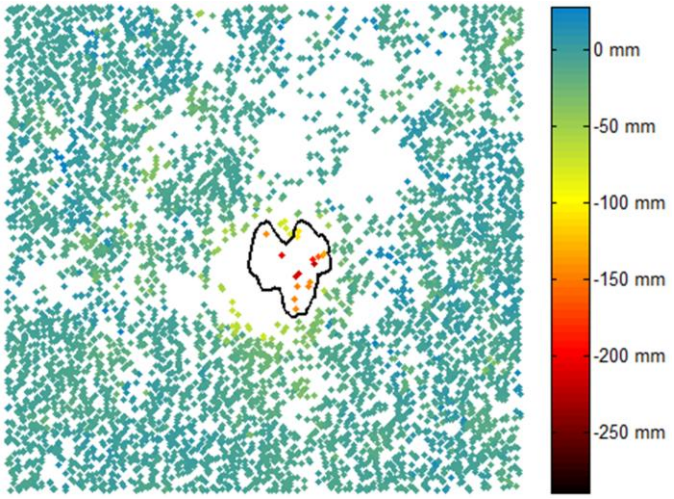

Figure 2. Sinkhole 1 Segmentation

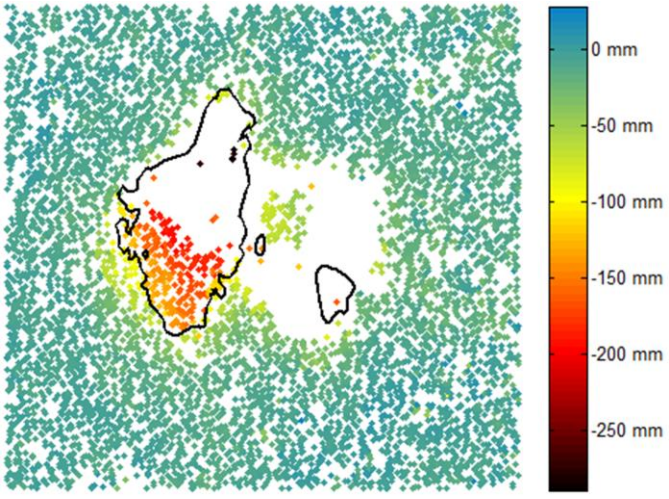

Figure 1. Sinkhole 2 Segmentation

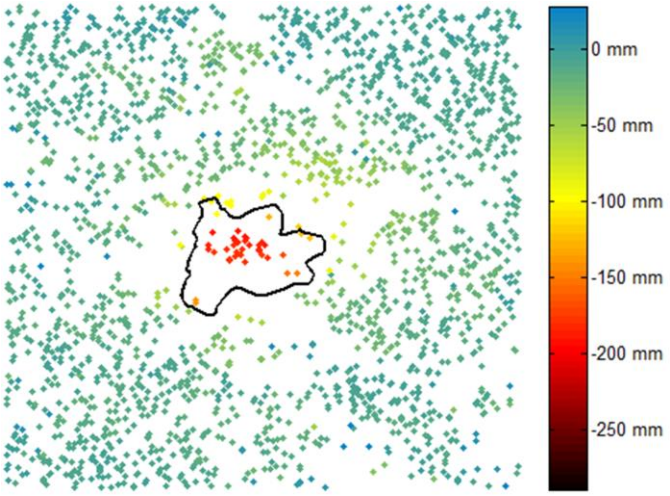

Figure 3. Sinkhole 3 Segmentation

- a large displacement difference between two vertices
- a displacement magnitude which resides within a narrow, sufficiently negative band of displacements

For each edge, e_i, connecting vertices (v_{i1},v_{i2}) with displacements (d_{i1},d_{i2}), average displacement d_{avg}, and average coherence coh_{avg}, we arrive at:

$$E_{band}(v_{i1}, v_{i2}) = \begin{cases} 0 & \text{if } d_{low} < d_{avg} < d_{high} \\ min(|d_{high} - d_{avg}|, |d_{low} - d_{avg}|) & else \end{cases} \quad (6)$$

$$E_{diff} = \frac{1}{|d_{i2} - d_{i1}|} \quad (7)$$

$$E_{reliable} = \frac{1}{coh_{avg}} \quad (8)$$

$$E_{length} = length(e_i) \quad (9)$$

E_{length} is included to give priority to cuts that pass through shorter, and thus more accurate, edges, in turn increasing the accuracy of the cut. In order to facilitate a meaningful combination of these energies, each energy is normalized to the same mean and standard deviation.

The energy of an edge is given by

$$E = \alpha \cdot E_{band} + \beta \cdot E_{diff} + \gamma \cdot E_{reliable} + \delta \cdot E_{length} \quad (10)$$

where α, β, γ, and δ are inter-category weighting parameters. We omit any associativity parameters in the composite energy function, as we do not wish to explicitly encourage spatial coherence. In fact, some points in the dataset may represent physical areas which are actually quite large. If such a point has associated data and trends with surrounding pixels accurately indicating that a sinkhole may be forming, the algorithm should not discourage a cut around that point and in the process miss a segmentation of a potential sinkhole-forming region.

Once this conglomerate energy function is achieved, we then find minimum-energy graph cuts. The number of cut contours is determined by the number of statistically significant energy minima present after each cut. Lastly, we fit a spline to these cuts, using the midpoint of each edge as interpolant points—these splines are the final result of the segmentation.

IV. Results and Discussion

A. Dataset

We analyzed a sparse, non-uniform point cloud derived from 22 InSAR images acquired from June 1992 – February 1998 via the SqueeSAR™ processing algorithm (credit: TRE Canada, Inc.). The point cloud contains 93,513 points; for each point, there is a displacement time series containing 21 entries, coherence, elevation, velocity, acceleration, area represented, and a few other miscellaneous attributes. The area of study resides in Wink, Texas, and occupies 55.37 square kilometers. There are two large, known sinkholes contained in this dataset: one which collapsed before the acquisition of data, in June 1980 (referred to as sinkhole 1), and one which collapsed after the images were acquired, in May 2002 (sinkhole 2).

B. Results

Our method was applied to three areas of interest within the previously described dataset: points proximal to sinkholes 1 and 2, as well as those close to a third, suspected sinkhole. Figs. 1-3 show the segmentation achieved for each subset (black splines) plotted against the point cloud used (color-mapped by displacement). We used cumulative displacement data selected from an arbitrarily late entry in the displacement time series in order to reflect long-term ground behavior. This displacement has a range of -289 mm to 95.5 mm, and a mean of -8.64 mm. For all subsets, the following parameters were employed: α = 0.1, β = 1, γ = 2, λ = 0.5, d_{low} = -115 mm, d_{high} = -99 mm.

This segmentation of possible sinkhole-forming regions for sinkholes 1 and 2 is also shown alongside their respective ground truth (Fig. 4 and Fig. 5, respectively). The segmentation given by the graph-cut method is shown in black, while the blue polygon represents the true extent of each collapsed sinkhole. As shown in Table 1, we capture about 27% of sinkhole 1, and 94% of sinkhole 2. We do not capture a significant portion of sinkhole 1; however, this sinkhole had already collapsed (and mostly filled with water) before the acquisition period even began, and thus presented poor scattering characteristics for incident radar energy. This resulted in a lack of data over much of the area in and surrounding sinkhole 1. Sinkhole 2, on the other hand, collapsed after the data collection period ended—thus, we had sufficient point density to provide a more robust detection.

TABLE I. Sinkhole Detection vs. Ground Truth

	Total Area of Sinkhole	***Area Within Segmentation***	***% Detected***
Sinkhole 1	8,476 m^2	2,306 m^2	27.20%
Sinkhole 2	5,098 m^2	4,775 m^2	93.67%

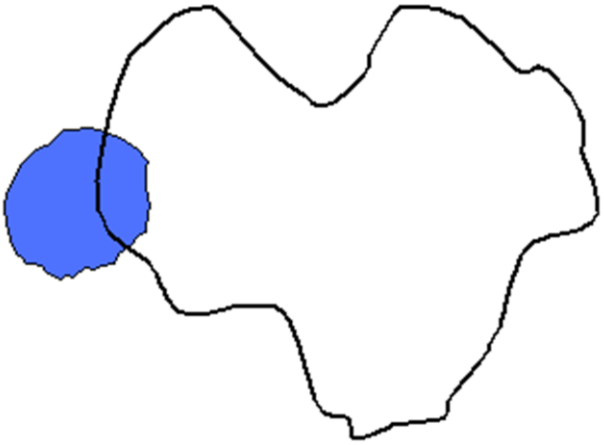

Figure 5. Sinkhole 1 Ground Truth

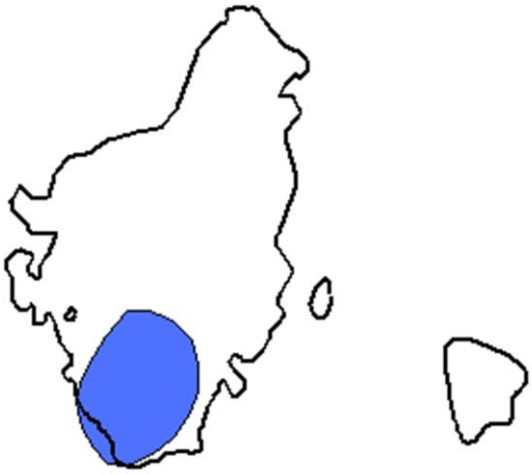

Figure 4. Sinkhole 2 Ground Truth

V. CONCLUSION

In this paper, we presented a method for the automatic detection of possible sinkhole-forming regions via graph-cut segmentation of non-uniform, sparse data. Our energy function was derived from multiple independent energies tailored towards accurately locating the boundaries of spot-like, subsiding regions.

Future work directed in this pursuit includes: optimizing the exact cut location on an edge (rather than simply using the midpoint), including temporal analysis (coherence of detection regions over time), estimating the probability of collapse, assigning risk factors dependent upon soil types and infrastructure present, and including additional factors indicative of spot-like subsidence behavior to the edge energy function.

REFERENCES

[1] E. Zebker (Ed.), "InSAR Workshop Summary Report," Jet Propulsion Laboratory – California Institute of Technology, 2004.

[2] F. Yang, P. A. Mlsna, and P. G. Geissler, "Gaussian-Based Filters for Detecting Martian Dust Devils," *Image Analysis and Interpretation, 2006 IEEE Southwest Symposium on*, pp. 46-50, doi: 10.1109/SSIAI.2006.1633719.

[3] K. Tomiyasu, "Tutorial review of synthetic-aperture radar (SAR) with applications to imaging of the ocean surface," *Proceedings of the IEEE*, vol. 66(5), pp. 563-583, May 1978.

[4] P. A. Rosen, et al., "Syntetic Aperture Radar Interferometry," *Proceedings of the IEEE*, vol.88(3), pp. 333-382, Mar. 2000.

[5] A. K. Gabriel, R. M. Goldstein, and H. A. Zebker, "Mapping Small Elevation Changes Over Large Areas: Differential Radar Interferometry," *Journal of Geophysical Research*, vol.94(B7), pp. 9183-9191, July 1989.

[6] H. A. Zebker, and J. Villasenor, "Decorrelation in Interferometric Radar Echoes," *IEEE Transaction on Geoscience and Remote Sensing*, vol.30(5), pp. 950-959, Sept. 1992.

[7] A. Ferretti, C. Prati, and F. Rocca, "Permanent Scatterer in SAR Interferometry," *IEEE Transaction on Geoscience and Remote* Sensing, vol.39(1), pp. 8-20, Jan. 2001.

[8] A. Ferretti, A. Fumagalli, F. Novali, C. Prati, F. Rocca, and A. Rucci, "A New Algorithm for Processing Interferometric Data-Stacks: SqueeSAR," *IEEE Transaction on Geoscience and Remote Sensing*, vol.49(9), pp.3460-3470, Sept. 2011.

[9] J. Shi, and J. Malik, "Normalized cuts and image segmentation," *IEEE Trans. Pattern Anal. Mach. Intell.*, vol. 22(8), pp. 888-905, Aug. 2000.

[10] X. Lin, B. Cowan, and A. Young, "Model-based Graph Cut Method for Segmentation of the Left Ventricle," *IEEE Eng. In Medicine and Biology.*, vol. 27, pp. 3059-3062, Jan. 2006